AIAA JOURNAL
Vol. 39, No. 10, October 2001

Lowering Thermal Residual Stresses in Composite Patch Repairs in Metallic Aircraft Structure

J. Cho* and C. T. Sun†
Purdue University, West Lafayette, Indiana 47907-1282

Thermal residual stresses induced by the bonding of composite patch repairs cause adverse effects on the fatigue performance of patch repairs. The reduction of residual stresses was attempted by modifying the cure cycle of the adhesive, FM73M. An effective temperature drop ΔT_{eff} was determined to quantify thermal residual stresses. Various cure cycles for the adhesive were investigated empirically to determine the cure time and cure temperature combination that can achieve a 100% degree of cure and the desired mechanical properties. An efficient two-step cure cycle was developed for bonding composite patches to cracked aluminum plates. The effect of reduced residual stress on the fatigue life of cracked aluminum plates repaired with symmetrical composite patches was investigated experimentally and numerically.

I. Introduction

LIKE other load-bearing structures, aging aircraft may contain damaged or cracked structural components resulting from fatigue and corrosion during service, and the degraded structural components must be replaced or repaired to extend their service lives. Because of the superior properties of advanced fiber composites and the maturing adhesive bonding technology, composite patch repair is now recognized as an efficient and economical repair technology.[1] Because bonded repairs using high-performance composite materials offer high efficiency and enhanced structural integrity, extensive works of composite patching on metallic aircraft components have been performed and reported. Examples include Hercules aircraft wings, Mirage wing skins, an Orion fuselage skin, an F-111 wing pivot fitting, a B-767 lower fuselage, and an MD-82 leading-edge slat that were repaired with boron/epoxy patches.[1,2] Because high-performance adhesives used in bonding require elevated cure temperatures, significant thermal residual stresses in the repair result from the mismatch of thermal expansion coefficients between the composite patch and the cracked aluminum structure. The induced thermal residual stresses in the aluminum structure are tensile and tend to open the crack, thus inducing a substantial level of stress intensity at the crack tip. Evidently, the residual stresses can reduce the effectiveness of the patch on the fatigue performance of the patched structure.[3]

In general, thermal residual stresses in the metallic structure repaired with adhesively bonded composite patches can be reduced by lowering the bonding (curing) temperature. However, lowering the cure temperature of the adhesive can yield adverse effects on the degree of cure of the adhesive and, as a result, yield poorer mechanical properties of the repair. Moreover, lower cure temperatures require longer cure time to achieve, if ever, the same degree of cure with a high cure temperature. In this study, an experimental investigation of various cure cycles for the adhesive was performed to find an efficient cure time and cure temperature combination that can achieve a 100% cure and the desired mechanical properties.

A two-step bonding cycle was selected to reduce thermal residual stresses and to study its effectiveness on the fatigue life of composite patch repairs. Fatigue lives of double-sided patch repairs fabricated with the bonding cycle recommended by the manufacturer (Cytec Industries, Inc.) of FM73M and by the two-step cycle, respectively, were modeled and compared. The experimental result indicated that lowering thermal residual stresses can be achieved by the two-step bonding cycle and can significantly prolong the fatigue life of the aluminum panel repaired with composite patches.

In actual applications of composite patch repairs, the cocuring procedure that involves the use of prepreg composite tapes during bonding is often followed. In this study, precured composite patches were used to avoid the potential complications that could arise from curing of the composite.

II. Reduction of Thermal Residual Stress

A. Effective Stress-Free Temperature

Thermal residual stresses in laminates after curing are usually calculated by using the elastic laminated plate theory in conjunction with an assumed temperature drop ΔT, which is defined as the temperature difference between the stress-free temperature and the service temperature. Because the physical and mechanical properties of the composite and adhesive are not constant during the bonding cycle, the stress-free temperature is not the same as the curing temperature. Thus, an effective temperature drop ΔT_{eff} needs to be determined. In this study, two methods based on curvature and strain measurements were employed to determine ΔT_{eff}.

1. *Measurement of Curvature and Residual Strain*

Two composite systems, carbon/epoxy (IM7/954-2A) and boron/epoxy (boron/5521), and 1.6- and 0.8-mm-thick 2024-T3 aluminum panels were considered. For the case of double-sided bonding, only the 1.6-mm aluminum panel was used. The properties of the selected materials are given in Table 1. Six-ply unidirectional composite laminate panels were fabricated first and then cut with a water jet to 127×76.2 mm in size. To bond the composite panel to the 2024-T3 of the same size, the surfaces of both materials must be treated properly.[4] Composite patches were bonded to the host aluminum with adhesive FM73M. One-sided and double-sided bondings were made with the selected bonding cycle.

After bonding, curvature occurred in the panel bonded with composite on one side. The curvature was obtained from the radius of the specimen measured with a Mitutoyo three-dimensional coordinate measuring machine. The measured curvature was then used to estimate the ΔT_{eff} with the aid of laminated plate theory.

Parallel to the measurement of curvatures, the residual strain in the composite of the aluminum/composite specimen after bonding was also measured by dissolving the aluminum plate. A strain gauge (Micro-Measurement Type EA-13-125AC-350) was mounted on the composite patch, and initial output of the strain gauge was recorded before the specimen was put into the sodium hydroxide (NaOH) solution. In addition, the strain gauge was sealed with silicon–rubber to protect it from the caustic solution. This measured residual strain in the composite was also used to determine ΔT_{eff}.

Received 7 August 2000; revision received 4 January 2001; accepted for publication 18 January 2001.

*Graduate Student, School of Aeronautics and Astronautics.
†Neil Armstrong Distinguished Professor of Aeronautical and Astronautical Engineering, School of Aeronautics and Astronautics. Fellow AIAA.

Table 1 Properties of used materials

Property	IM7/954-2A	Boron/5521	Al 2024-T3	FM73M
$E_1(E)$, GPa	174.7	206.9	72	2.28
E_2, GPa	10.1	18.6	——	——
G_{12}, GPa	5.8	6.2	——	——
$\nu_{12}(\nu)$	0.29	0.21	0.3	0.34
α_1 (10^{-6}/°C)	−0.3	4.5	23	——
α_2 (10^{-6}/°C)	30	23	23	——

2. Determination of ΔT_{eff}

Measured curvatures and residual strains from the aluminum/composite specimens were analyzed using the thermoelastic laminated plate theory. The patched specimen is considered as a laminated plate consisting of composite, aluminum, and adhesive layers. For free thermal expansion, the plate constitute equations reduce to[5]

$$\Delta T \begin{Bmatrix} N^T \\ M^T \end{Bmatrix} = \begin{bmatrix} A & B \\ B & D \end{bmatrix} \begin{Bmatrix} \varepsilon^0 \\ \kappa \end{Bmatrix} \tag{1}$$

where

$$\{N^T\} = \sum_{k=1}^{n} [\bar{Q}]_k \{\alpha\}_k (z_k - z_{k-1})$$

$$\{M^T\} = \sum_{k=1}^{n} [\bar{Q}]_k \{\alpha\}_k \left(z_k^2 - z_{k-1}^2\right)$$

are plate resultant forces and moments, respectively, for free thermal expansion or contraction; $\{\varepsilon^0\}$ and $\{\kappa\}$ are in-plane strains and curvatures, respectively; $\left[\bar{Q}\right]_k$ is the stiffness matrix in the kth lamina; $(z_{k-1} - z_k)$ is the thickness region of the kth lamina in a laminated plate; and the elements in $\{\alpha\}$ are thermal expansion coefficients.

For the symmetrically patched laminate, $\{\kappa\} = 0$, and coupling stiffnesses vanish, that is, $B_{ij} = 0$. Thus, from Eq. (1), ΔT_{eff} can be calculated with measured ε_x^0 from Eq. (2):

$$\Delta T_{\text{eff}} = \left(A_{11} \big/ N_x^T\right) \varepsilon_x^0 \tag{2}$$

For the one-sided patched laminate, $B_{ij} \neq 0$ and $\{\kappa\} \neq 0$. After some manipulation with Eq. (1), ΔT_{eff} is related to the measured residual strain and curvature as follows:

$$\Delta T_{\text{eff}} = \left(R_{11}^{\varepsilon} \big/ P_1^{\varepsilon}\right) \varepsilon_x^0 \tag{3}$$

$$\Delta T_{\text{eff}} = \left(R_{11}^{\kappa} \big/ P_1^{\kappa}\right) \kappa_x \tag{4}$$

where

$$\{P^{\kappa}\} = \{M^T\} - [B][A]^{-1}\{N^T\}, \qquad \{P^{\varepsilon}\} = \{M^T\} - [D][B]^{-1}\{N^T\}$$

$$[R^{\kappa}] = [D] - [B][A]^{-1}[B], \qquad [R^{\varepsilon}] = [B] - [D][B]^{-1}[A]$$

Table 2 lists the evaluated ΔT_{eff} for the recommended bonding cycle (121°C for 1 h), which were determined from five specimens for each case. Consistent results for ΔT_{eff} from the curvature and residual strain measurements are evident for both one-sided and double-sided bonding configurations and for both composite systems. Hence, it is reasonable to conclude that ΔT_{eff} depends mainly on the cure cycle of the adhesive. The curvature measurement method and the IM7/954-2A carbon/epoxy composite were henceforth chosen to determine ΔT_{eff} for modified cure cycles. For the recommended cure cycle of FM73M, the average value of ΔT_{eff} was found to be −90°C.

B. Effect of Cure Temperature and Cure Time on Properties of FM73M

The recommended cure cycle for FM73M is a one-step cure, as shown in Fig. 1. Although cure temperature, cure time, cool-down rate, heat-up rate, and pressure may affect curing of the adhesive, cure temperature and cure time are regarded as the dominant parameters. Hence, the modification of the cure cycle of FM73M was undertaken by changing these two parameters.

Table 2 Comparison of ΔT_{eff} for different bonding configurations and composites

	Single-sided bonding		Double-sided
121°C cure	Curvature, °C	Strain, °C	bonding strain, °C
IM7/954-2A	−89	−88	−94
Boron/5521	−89	−87	——

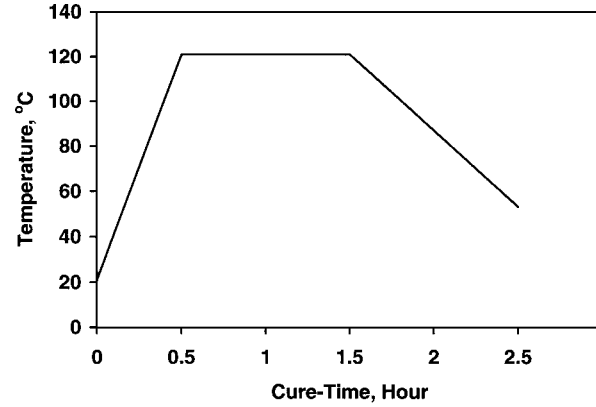

Fig. 1 Autoclave cure cycle of FM73M adhesive.

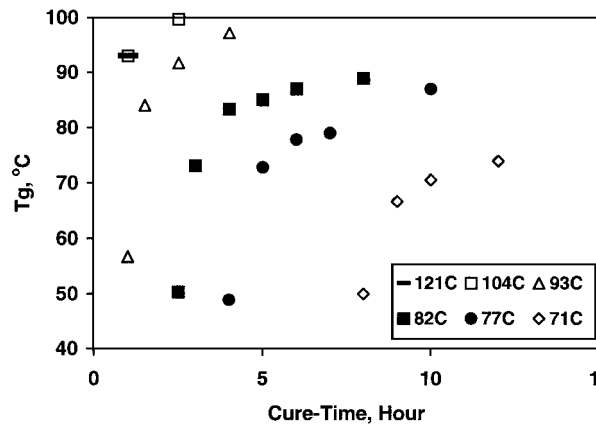

Fig. 2 Development of T_g for various cure cycles.

1. Effect on Glass Transition Temperature T_g and Mechanical Properties

The degree of cure resulting from a cure cycle was investigated with respect to the development of T_g, which is known as a useful quantity characterizing the progression of cure in thermoplastics and thermosets. The T_g can be determined readily by observing the temperature region in which a significant change in mechanical properties takes place. In this study, the temperature region where a drastic change in deformation under a constant load occurs was determined and taken as the T_g.

FM73M panels 1.4 mm thick were cured in an autoclave according to the chosen cure cycles. The cured panels were cut into coupon specimens of 25.4 × 203.2 mm. The glass transition temperature was determined following the standard method recommended by the American Society for Testing and Materials E1824 (Ref. 6). The T_g of FM73M cured at the recommended cycle was used to determine whether or not a specimen cured at a modified cycle achieved the complete degree of cure. Figure 2 shows the experimental results for different combinations of cure temperatures and times. For each data point, two specimens were tested and the average value was taken.

It has been reported that mechanical properties of a polymer depend on its degree of cure.[7] Thus, to investigate the change of mechanical properties with respect to the degree of cure, the elastic modulus and ultimate tensile strength of 10-layer FM73M cured in modified cure cycles were measured. The cured FM73M was cut with a water jet to 25.4 × 203.2 mm. Longitudinal strains were

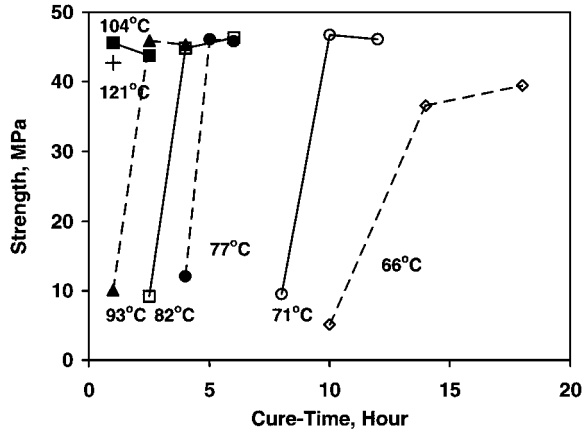

Fig. 3 Development of tensile ultimate strength.

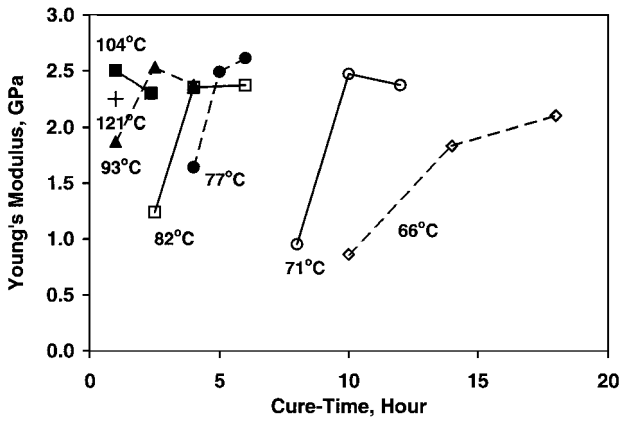

Fig. 4 Development of Young's modulus.

measured. Tension tests were performed at room temperature with a strain rate of 10^{-4}/s. Load vs strain was monitored continuously to failure. The ultimate tensile strengths and Young's moduli for specimens cured with various modified cure cycles are presented in Figs. 3 and 4, respectively. In Figs. 3 and 4, each data point denotes the average of three specimens tested.

The effects of modified cure parameters (cure temperature and time) on the development of T_g and tensile mechanical properties can be observed in Figs. 2–4. Note that, as cure temperature decreases, the development of T_g and tensile mechanical properties becomes slower, and the tensile mechanical properties increase as T_g increases. However, no such clear relation between cure time and T_g or tensile mechanical properties was found. Considering cure temperatures 93 and 82°C in Figs. 3 and 4, for instance, the fully developed tensile strengths and elastic moduli were obtained at 2.5 and 4 h, respectively. However, the 100% degree of cure was not achieved, as shown in Fig. 2. In view of this, we should recognize that, even if the desired mechanical properties are obtained at room temperature, it does not mean that a 100% degree of cure is also achieved. To amplify this point, another adhesive acceptance test is needed to determine whether a modified cure cycle has achieved both a 100% degree of cure and fully developed mechanical properties.

2. Lap-Shear Strength at Elevated Temperatures

The lap-shear test is known as a useful method for quantitatively comparing the quality of various adhesives and is one of the standard adhesive tests. Single-lap specimens are the most widely used specimens for comparative studies involving adhesives and bonded products because they are economical, practical, and easy to fabricate. Thus, single-lap tests have been commonly used for comparing and selecting adhesives or bonding processes.[8] The test should be performed at room temperature as well as at the highest service temperature. The range of the service temperature of FM73M (Ref. 1) is from −55 to 82°C. Additionally, for airworthiness requirements,[9] the highest temperature for aircraft structure is 110°C. Hence, 21, 82, and 110°C were selected as the test temperatures in this study. Strengths obtained from specimens cured with various modified cure cycles were compared with those of the specimen cured with the recommended cure cycle. From this comparison, satisfactory modified cure cycles were found.

Table 3 Lap-shear strengths (MPa) at various temperatures and T_g for selected cure cycles

Cure temperature/duration	T_g, °C	21°C	82°C	110°C
121°C/1 h (recommended)	93	25.37	21.86	14.80
104°C/1 h	93	25.00	22.16	14.90
93°C/2.5 h	91	27.13	22.59	12.68
93°C/4 h	97	24.51	22.76	14.13
82°C/4 h	83	25.16	17.36	7.43
82°C/8 h	89	23.32	21.49	11.49
82°C/10 h	——	26.28	22.73	11.46
77°C/6 h	78	25.44	15.43	5.25
77°C/10 h	87	25.17	20.22	9.04
77°C/5 h + 104°C/1 h	——	26.60	23.23	14.63
82°C/4 h + 104°C/0.5 h	——	25.13	22.54	15.50

In the lap-shear test, aluminum alloy 6061-T6 was used as the adherend. As recommended in the standard method,[8] the thickness and length of the adherend were chosen to be 1.6 and 101.6 mm, respectively. Aluminum adherends were bonded after the proper surface treatment with a 12.7-mm overlap length. The bonded specimen was cut with a water jet to the width of 25.4 mm. Tests were conducted at a cross-head speed of 1.27 mm/min.

The lap-shear strengths obtained from the lap-shear tests for various modified bonding (cure) cycles are presented in Table 3. In each case, three specimens were tested, and the average strength was taken. The glass transition temperatures for cure cycles obtained from Fig. 2 are also listed. Note that the fully developed lap-shear strength at room temperature can be obtained before a 100% degree of cure is reached, as illustrated by the 82°C/4 h cure cycle. All cases tested indicate that, once the T_g of 93°C is reached, the lap-shear strength at 110°C also reaches its full strength. On the other hand, if the lap-shear strength at 110°C of a specimen cured at a modified cure cycle is fully developed, this cure cycle will yield a 100% degree of cure for the FM73M adhesive. The two-step cure cycles listed in Table 3, thus, will yield a 100% degree of cure at the end of the cycle.

One-step cycles require either a long cure time or a high cure temperature to obtain the desired T_g and mechanical properties. Long cure time is undesirable economically. On the other hand, high cure temperatures would give rise to high thermal residual stresses.

C. Two-Step Cure Cycle

White and Hahn,[7] who investigated laminates of polymer composites, observed that, after postcure, thermal residual stresses increased slightly from those after the primary cure cycle. This increase could be explained by the increase in mechanical properties. This phenomenon led to the possibility of adding a cure cycle following the primary cycle to achieve the effect of postcure. White and Hahn[7] also reported that the development of thermal residual stresses was dependent on the development of the degree of cure in the primary cure cycle.

In the present study, the two-step bonding (cure) cycle was investigated for the use for composite patch repairs. The present two-step cure cycle involves a lower cure temperature preceding a higher cure temperature. The two-step cure cycle is depicted in Fig. 5. Although it is not necessary to achieve the 100% degree of cure in the first step, 77°C was chosen as the minimum cure temperature for the first-step cure because the development of T_g becomes exceedingly slow as the cure temperature falls below 77°C. Moreover, cure temperatures lower than 77°C would take a long time to attain the desired mechanical properties, as indicated in Fig. 3. Thus, 77, 82, and 88°C were selected for the first-step cure temperature. For the second-step cure temperature, it is required that the temperature be high enough to fully develop the mechanical properties within a short time. For this reason, 104 and 93°C were selected. Second, by taking the cure time into account, 104°C was selected for the

Table 4 ΔT_{eff} for two-step cure cycles

Two-step cure cycle	ΔT_{eff}, °C
77°C/5 h + 104°C/1 h	−61
77°C/6 h + 104°C/1 h	−51
82°C/3.5 h + 104°C/1 h	−57
82°C/4 h + 104°C/0.5 h	−53
82°C/5 h + 104°C/1 h	−53
88°C/3.5 h + 104°C/1 h	−62
88°C/4 h + 104°C/1 h	−62

Table 5 Reduction of thermal residual stresses

Bonding cycle	ΔT_{eff}, °C
121°C/1 h	−90
82°C/4 h + 104°C/0.5 h	−53

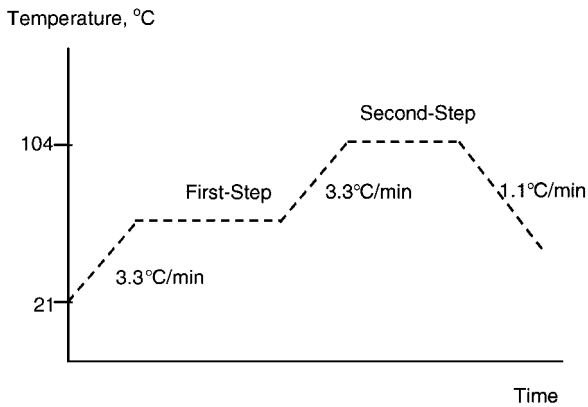

Fig. 5 Two-step cure cycle.

second-step cure temperature. The applied pressure, heat-up rate, and cool-down rate were kept the same as the one-step cure cycle recommended by the manufacturer.

With the curvature measurement method described in Sec. II.A, ΔT_{eff} for a number of trial two-step cure cycles were determined with the results listed in Table 4. Note that ΔT_{eff} decreases as degree of cure increases and cure temperature decreases in the first-step cure. When ΔT_{eff} and cure time are considered, the 82°C/4-h plus 104°C/0.5-h two-step cure cycle appeared to be an efficient combination. This two-step cure cycle, which yielded a 40% reduction of thermal residual stresses, as summarized in Table 5, was selected for further study of fatigue behavior of the composite repair.

III. Fatigue Life of Composite Patch Repair

A. Experimental Observation

The fatigue strength of composite patch repairs was studied. The aluminum alloy and the composite used in this work were 2024-T3 and AS4/3501-6, respectively. Properties of AS4/3501-6 are listed in Table 6. First, a four-layer unidirectional laminate of AS4/3501-6 carbon/epoxy composite was fabricated. The composite laminate was cut with a water jet to 63.5 × 76.2 mm. The aluminum plate was 88.9 × 254 mm. Before bonding, a center crack was cracked with the water jet and then sharpened with a jeweler's saw. Subsequently, a fatigue crack was initiated to a total crack length of 15 mm. The specimen surfaces were then treated for bonding. Bonding was done with the adhesive FM73M in an autoclave with the manufacturer-recommended cure cycle and the selected modified cure cycle (82°C/4 h plus 104°C/0.5 h). A patched specimen is illustrated in Fig. 6.

The fatigue test was performed with 6-Hz loading frequency. A positive loading ratio ($R_{\text{load}} = 0.01$) was selected to avoid buckling. The peak loading stress was 120.5 MPa, which is 30% of the yield stress of the host aluminum plate. The ultrasonic C-scan was conducted to detect and record crack length. The through-transmission technique was performed with 10-MHz transducers.

Table 6 Material properties of AS4/3501-6

Property, GPa	AS4/3501-6
E_1	142
E_2	10.3
E_3	10.3
G_{12}	7.2
G_{13}	7.2
G_{23}	3.2
ν_{12}	0.27
ν_{13}	0.27
ν_{23}	0.49
α_1 (10^{-6}/°C)	−0.9
α_2 (10^{-6}/°C)	27
α_3 (10^{-6}/°C)	27

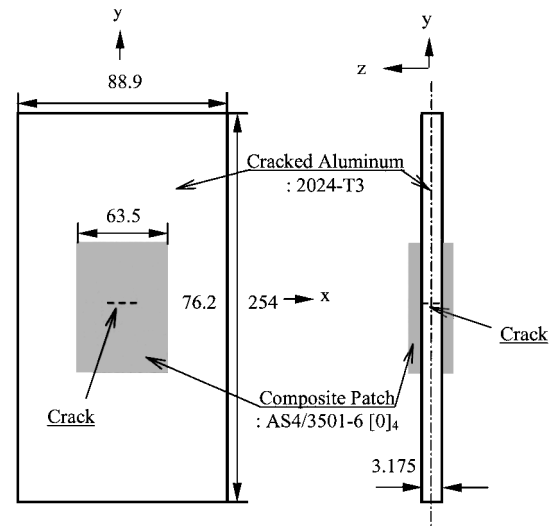

Fig. 6 Specimen of the double-sided repair; millimeters.

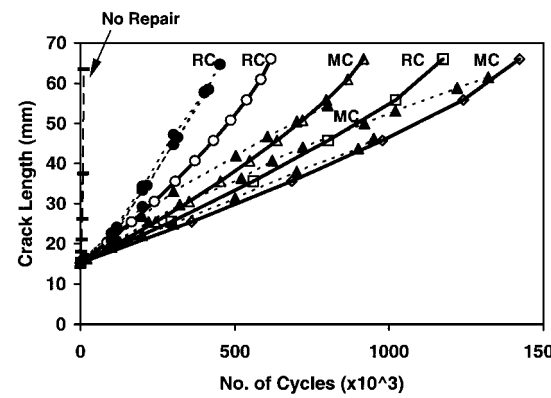

Fig. 7 Experimental and numerical results for fatigue crack growth: for recommended cure cycle (RC): ●, experiment; ○, prediction with strain rate effect; and □, prediction with linear elasticity; for modified cycle (MC): ▲, experiment; △, prediction with strain rate effect; and ◇, prediction with linear elasticity.

Fatigue lives for repaired and unrepaired specimens are presented in Fig. 7. Note that the modified two-step cure cycle significantly prolonged the fatigue life of the composite patch repair as compared with that of the recommended cure cycle. Note that the fatigue data for the specimens of the modified cure cycle exhibit a greater scatter. This could be the result of the use of the ultrasonic measurement that does not give the precise location of the crack tip.

B. Finite Element Modeling

To predict the fatigue crack growth in the aluminum panel repaired with composite patches, the stress intensity factor of the aluminum crack must be calculated. The stress intensity factor was derived

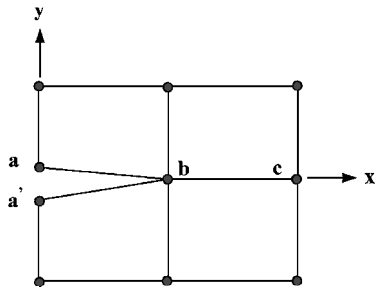

Fig. 8 Two-dimensional finite element model for cracked aluminum plate.

from the strain energy release rate, which was calculated using the modified crack closure technique.[10,11] Based on the modified crack closure technique, the total strain energy release rate for mode 1 over the total thickness of the aluminum plate is

$$\bar{G}_I = (1/2\Delta a)\left\{F_y^b\left(u_y^a - u_y^{a'}\right)\right\} + (1/2\Delta a)\left\{M_x^b\left(\psi_x^a - \psi_x^{a'}\right)\right\} \quad (5)$$

where F_y^b and M_x^b are the nodal force and moment at node b, respectively, and u_y^a and ψ_x^a are the opening displacement and rotation at node a, respectively, as illustrated in Fig. 8. For the double-sided symmetric repair, the contribution of the second term in Eq. (5) is negligible. For double-sided symmetric patch repairs under mode 1 loading, the stress intensity factor can be derived from $\bar{G}_I$ as[10]

$$K_I = \sqrt{\bar{G}_I E_{\text{al}}/t_{\text{al}}}$$

where t_{al} and E_{al} are thickness and Young's modulus of the aluminum plate, respectively, and K_I is stress intensity factor.

To evaluate the stress intensity factor, this finite element model was established with the commercial finite element package ABAQUS.[12] In this model, the cracked aluminum plate and composite patches were represented by Mindlin plates. This technique has been shown to provide an accurate and efficient analysis of patch repairs.[10] For the Mindlin plate, a four-node shell element was used. For the adhesive, a layer of eight-node three-dimensional brick elements was used. Two layers of three-dimensional elements were found to provide little improvement in the solution.[13] For compatibility along the interfaces, constraint equations were imposed to relate the displacements of the element nodes between the patch–adhesive and the adhesive–aluminum interfaces according to Mindlin plate theory (see Ref. 10). In addition, to ensure a sufficiently small Δa in Eq. (5), it is recommended to use the ratio $\Delta a/a$ less than 0.05 (Ref. 14). In the present model, the ratio $\Delta a/a$ less than 0.03 was made with uniform Δa size.

Because of symmetry, a quadrant of the repair area with one-half of the thickness of the aluminum plate was modeled (see Fig. 6). Initially, the effective temperature drop ΔT_{eff} was applied to model the thermal residual stresses resulting from bonding. Subsequently, the grip condition was applied at the boundary of the aluminum plate. This was achieved by setting the rotations and the displacement in the z direction to zero. In addition, the displacements in the x and y directions at the grip edge were set equal using linear constraint equations.

Because FM73M is highly nonlinear and strain rate dependent,[15] a rate-dependent nonlinear constitutive model for the adhesive should be employed. The strain rate in the adhesive must be known first to select the appropriate stress–strain curve for the adhesive in the analysis. Apparently, this required an iterative procedure.

First, the lower bound and the upper bound of the strain rate in the adhesive associated with the fatigue loading were estimated. The lower bound was obtained through the linear elastic analysis. For the upper bound, the nonlinear stress–strain curve of the adhesive at a very low strain rate was used. In this study, a quasi-static strain rate of 10^{-4}/s was adopted to estimate the upper bound. The adhesive was modeled as an isotropic elastic–plastic material obeying the J_2 flow rule. In addition, thermal residual stresses resulting from the recommended bonding cycle were considered in the elastic–plastic analysis.

Maximum principal strains in the adhesive layer were calculated, and an elliptical region surrounding the aluminum crack was identified, in which the strains are much greater than the outside region. A

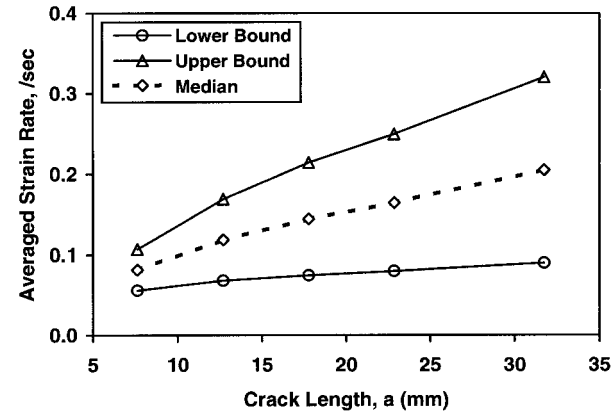

Fig. 9 Average strain rate in elliptic load transfer region vs crack length.

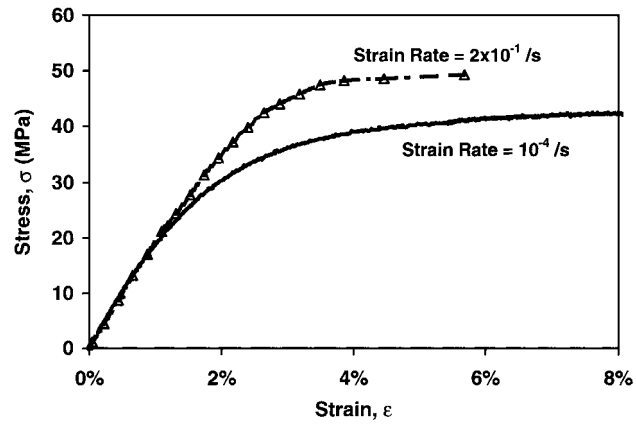

Fig. 10 Strain-rate-dependent behavior of FM73M.

principal strain of 0.2% was considered to determine the boundary of the region. For simplicity, the average strain rate in each element was taken as

$$\dot{\varepsilon} = (\varepsilon^{P\max} - \varepsilon^{P\min})/t \quad (6)$$

where $\varepsilon^{P\max}$ and $\varepsilon^{P\min}$ are the principal strains corresponding to the maximum and minimum of applied fatigue load, respectively, and t is half of each fatigue loading cycle time. An area-weighted average stain rate for the whole elliptical region was then obtained.

The estimated upper and lower bounds of the average strain rate in the ellitical region vs crack length are given in Fig. 9. The median value of the upper and lower bounds was taken as the representative strain rate for this region. To further simplify the analysis, the strain rate of 0.15/s corresponding to the median crack length was used for the analysis for the whole range of fatigue crack growth.

The nonlinear stress–strain curves for the fully cured FM73M for two strain rates were obtained from simple tension tests. The results are shown in Fig. 10. Because the representative strain rate in the loaded adhesive region was found to be 0.15/s, the stress–strain curve for FM73M at strain rate 0.2/s was used in the analysis. Subsequently, the stress intensity factor in the cracked aluminum was evaluated using the established finite element model with the stress–strain curve of FM73M.

For predicting fatigue crack growth with the calculated stress intensity factor, Walker's equation (see Ref. 16),

$$\frac{da}{dN} = \frac{C}{(1-R)^{m(1-\gamma)}}(\Delta K)^m \quad (7)$$

was used. In Eq. (7), C and m are constants implying material properties, γ is a constant obtained by curve fit of experimental data, and R is the ratio of the minimum to maximum stress intensity factor. All of the constants for aluminum alloy 2024-T3 in Eq. (7) are listed in Table 7. Numerical integration of Eq. (7) was performed with Simpson's rule.

Table 7 Constants for Walker's equation for aluminum alloy 2024-T3

Constant	Value
C, MPa $\cdot$ m$^{0.5}$	1.42×10^{-8}
m	3.59
γ	0.68

The model predictions and experimental results are shown in Fig. 7. The prediction obtained based on linear elasticity of the adhesive properties overestimates the fatigue life of the repair. This error is the result of overestimating the load transfer capacity of the adhesive. As shown in Fig. 7, the prediction is fairly good if the nonlinear rate dependent behavior of the adhesive is included in the model. On the other hand, although numerical results are not shown, the use of the quasi-static nonlinear stress–strain curve tends to underestimate the fatigue life of the composite patch.

IV. Conclusions

From the results of the present study, the following conclusions were obtained:

1) Thermal residual stresses can be reduced significantly with an efficient two-step bonding cycle by selecting cure parameters judiciously.

2) The reduction of thermal residual stresses from the modified bonding cycle can substantially improve the fatigue performance of the repair.

3) The strain rate effect on the nonlinear stress–strain behavior of the adhesive should be included in the model used in the analysis of the aluminum stress intensity factor.

Acknowledgment

This work was supported by the Air Force Office of Scientific Research through Grant F49620-98-1-0205 to Purdue University.

References

[1]Baker, A. A., and Jones, R., *Bonded Repair of Aircraft Structure*, Martinus–Nijhoff, Dordrecht, The Netherlands, 1988, pp. 1–18 and 162–172.

[2]Baker, A. A., and Chester, R. J., "Recent Advances in Bonded Composite Repair Technology for Metallic Aircraft Components," *Proceedings of the International Conference on Advanced Composite Materials*, Advanced Composite 93, Warrendale, PA, 1993, pp. 45–49.

[3]Lena, M. R., Klug, J., and Sun, C. T., "Composte Patches as Reinforcements and Crack Arrestors in Aircraft Structure," *Journal of Aircraft*, Vol. 35, No. 2, 1998, pp. 318–324.

[4]Cho, J., and Sun, C. T., "Lowering Thermal Stresses in Bonded Composite Repairs," *Proceedings of the 14th Technical Conference, American Society for Composites*, Technomic, Lancaster, PA, 1999, pp. 884–893.

[5]Daniel, I. M., and Ishai, O., *Engineering Mechanics of Composite Materials*, Oxford Univ. Press, New York, 1994, pp. 142–184.

[6]"Standard Test Method for Assignment of a Glass Transition Temperature Using Thermomechanical Analysis Under Tension," American Society for Testing and Materials, E1824, Vol. 14.02, West Conshohocken, PA, 1999.

[7]White, S. R., and Hahn, H. T., "Cure Cycle Optimization for the Reduction of Processing-Induced Residual Stresses in Composite Materials," *Journal of Composite Materials*, Vol. 27, No. 14, 1993, pp. 1352–1378.

[8]"Standard Test Method for Apparent Shear Strength of Single-Lap-Joint Adhesively Bonded Metal Specimens by Tension Loading (Metal to Metal)," American Society for Testing and Materials, D1002, Vol. 15.06, West Conshohocken, PA, 1999.

[9]Callinan, R. J., Sanderson, S., and Keeley, D., "Structural and Thermal F.M Analysis of Bonded Repair to an F-111 Wing," *ISASTI 96 Proceedings*, Jakarta, Indonesia, 1996, pp. 1027–1040.

[10]Sun, C. T., Klug, J. C., and Arendt, C., "Analysis of Cracked Aluminum Plates Repaired with Bonded Composite Patches," *AIAA Journal*, Vol. 34, No. 2, 1996, pp. 369–374.

[11]Rybicki, E. F., and Kanninen, M. F., "A Finite Element Calculation of Stress Intensity Factors by a Modified Crack Closure Integral," *Engineering Fracture Mechanics*, Vol. 9, 1977, pp. 931–938.

[12]*ABAQUS User's Manual*, Ver. 5.8, Hibbit, Karlson, and Sorenson, Inc., Pawtucket, RI, 1999.

[13]Klug, J. C., "Fracture and Fatigue of Bonded Composite Repairs," Ph.D. Dissertation, School of Aeronautics and Astronautics, Purdue Univ., West Lafayette, IN, Aug. 1997.

[14]Lena, M. R., "Repair and Reinforcement of Cracked Aluminum Plates with Adhesively Bonded Composite Patches," M.S. Thesis, School of Aeronautics and Astronautics, Purdue Univ., West Lafayette, IN, May 1995.

[15]Chiu, W. K., and Jones, R., "Unified Constitutive Model for Thermoset Adhesive, FM73," *International Journal of Adhesion and Adhesive*, Vol. 15, 1995, pp. 131–136.

[16]Dowling, N. E., *Mechanical Behavior of Materials (Engineering Methods for Deformation, Fracture and Fatigue)*, Prentice–Hall, Upper Saddle River, NJ, 1993, pp. 471–475.

A. Chattopadhyay
Associate Editor